

Observational constraints on the dynamics of the outer core

Chris Finlay

National Space Institute, Technical University of Denmark

Acknowledgements: Andy Jackson, Nicolas Gillet, Dominique Jault, Nils Olsen,
Sanja Panovska & Andrey Sheyko.

SEDI Meeting, Univ. Leeds, U.K., 3rd July 2012

Talk Outline

1. Introduction: The geomagnetic field and the core
2. Sources of magnetic field observations
3. Observation-based models of the core field and flow
4. The Holocene: past 10,000 yrs
5. The recent satellite era: past 13 yrs
6. Handling observational uncertainty: model covariances
7. Outlook

Talk Outline

1. Introduction: The geomagnetic field and the core
2. Sources of magnetic field observations
3. Observation-based models of the core field and flow
4. The Holocene: past 10,000 yrs
5. The recent satellite era: past 13 yrs
6. Handling observational uncertainty: model covariances
7. Outlook

Core dynamics and the geodynamo

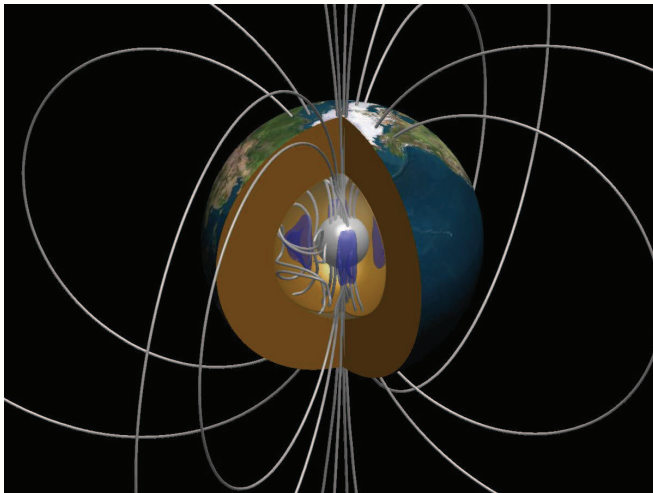


Fig 1.1: Schematic of the geodynamo process in Earth's core (credit: J. Aubert, IPGP)

- Long standing quest to understand how deep Earth processes generate the Earth's magnetic field and cause its evolution.

Temporal spectrum of geomagnetic field variations

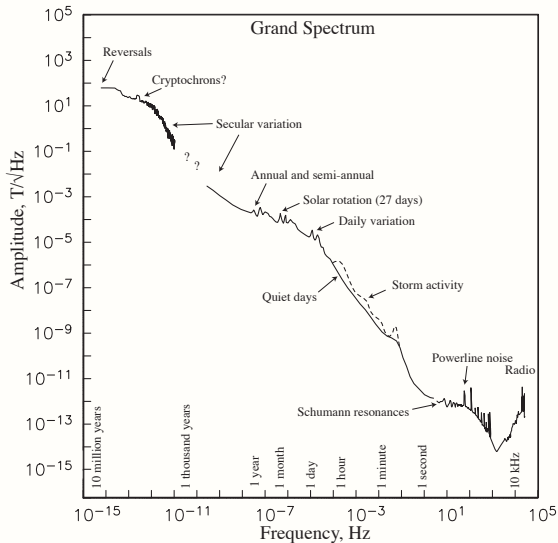


Fig 1.2: Temporal spectrum of magnetic field variability. From [Constable & Constable \(2004\)](#).

Observed geomagnetic field components

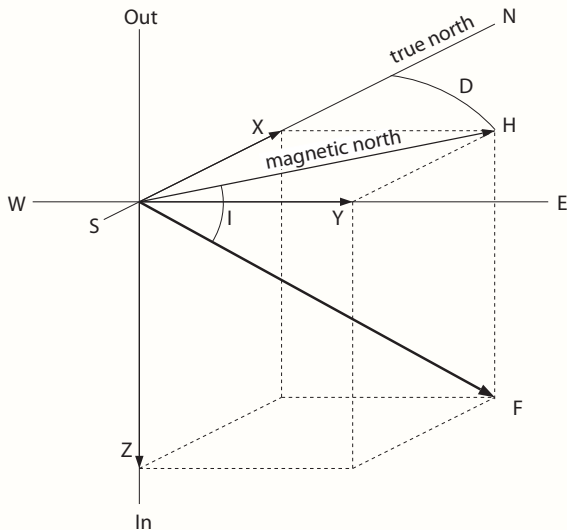


Fig 1.3: Commonly observed components of the geomagnetic field.

Sensitivity to the core surface magnetic field

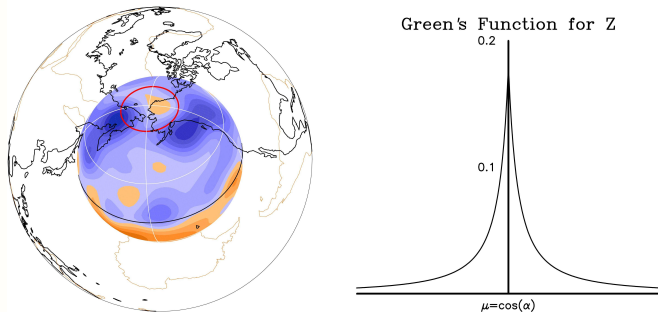


Fig 1.4: Z at core surface with Earth's surface shown together with the relevant Green's fns.

- Each observation is a weighted average of the core surface field (Gubbins & Roberts, 1983).

Sensitivity of D , I , F to B_r at the core surface.

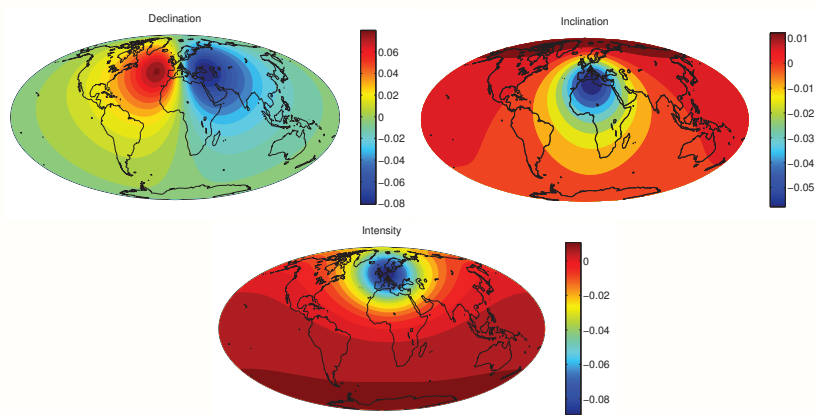


Fig 1.5: Averaging Kernel's showing sensitivity to B_r at core surface of D , I and F observations in central Europe at Earth's surface. (Plots courtesy of S. Panovska.)

Talk Outline

1. Introduction: The geomagnetic field and the core
- 2. Sources of magnetic field observations**
3. Observation-based models of the core field and flow
4. The Holocene: past 10,000 yrs
5. The recent satellite era: past 13 yrs
6. Handling observational uncertainty: model covariances
7. Outlook

Paleomagnetic observations

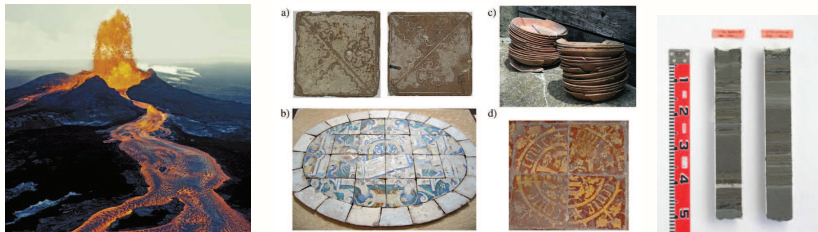


Fig 2.1: Examples of paleomagnetic data sources: Left: Lavas on Hawaii; Middle: archeological artifacts (Genevey et al., 2009); Right: a lake sediment core.

- Magnetization acquired by rocks during formation and artifacts during production records direction and intensity of the ancient field.

Temporal distribution of records in past 10kyrs

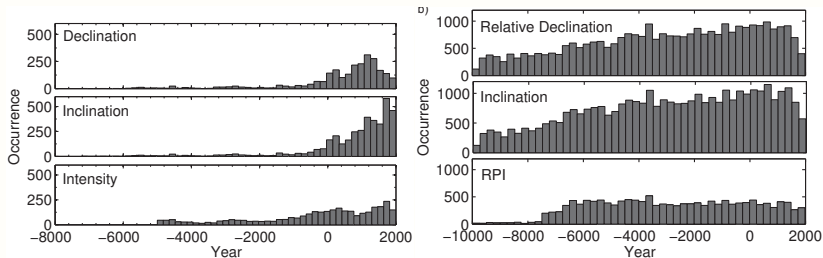


Fig 2.2: Time distribution of archeomagnetic and (left) and sediment (right) magnetic records during the past 10 kyrs (Korte et al., 2011), in 200 yr bins, courtesy of S. Panovska.

Distribution of sediment magnetic data (10 kyrs)

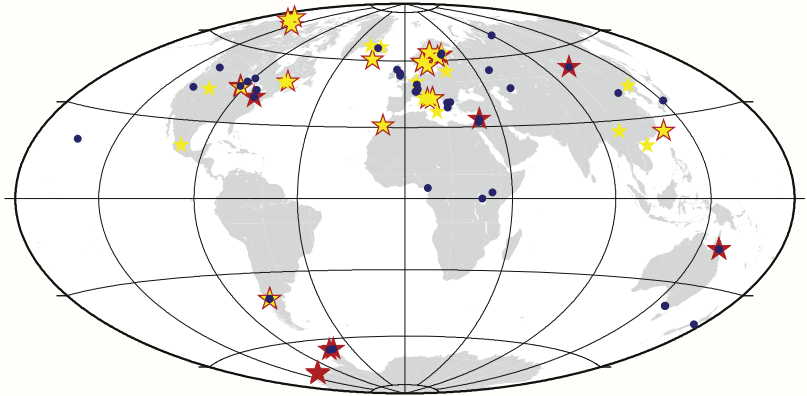


Fig 2.3: Locations of lake sediment records used to constrain the CALS10K model of [Korte et al. \(2011\)](#) spanning the past 10kyrs. Stars show locations of new records: Yellow stars for D/I, red stars or red borders around yellow stars for RPI. Locations of previously used records are blue dots.

Example: A famous Yorkshireman

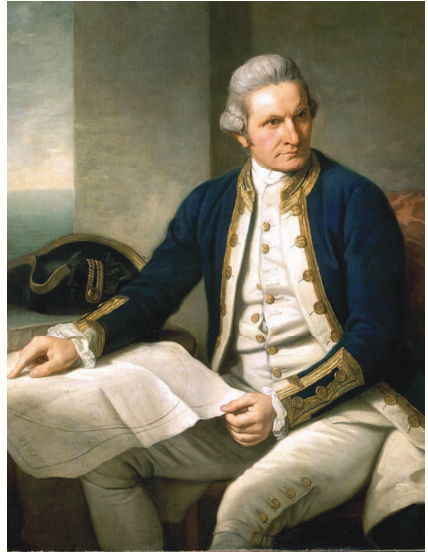


Fig 2.5: Reconstruction of Cook's Endeavour (left) and a portrait of him in 1776 (right).

Distribution of historical data (1770-1790)

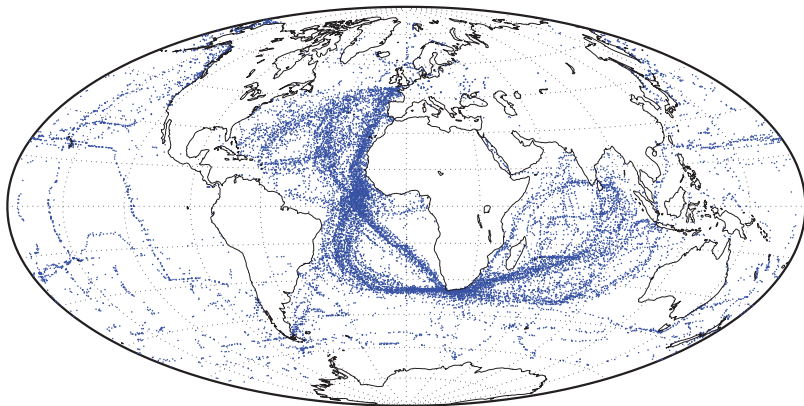


Fig 2.6: Locations of historical data (all components) between 1770 and 1790 from the [Jonkers et al. \(2003\)](#) database.

Ground magnetic observatories



Fig 2.7: Magnetic observatories at Eskdalemuir in the UK (top left), Kourou, French Guyana (top right), Qeqertarsuaq/Godhavn in Greenland (bot. left) and Hermanus in S. Africa (bot. right).

Example of instruments in use at observatories



Fig 2.8: D/I fluxgate theodolite, Danish fluxgate variometer, & Overhauser magnetometer (from ETHZ observatory in development on Gan, Maldives, courtesy of J. Velimsky).

Observatory distribution in 2010

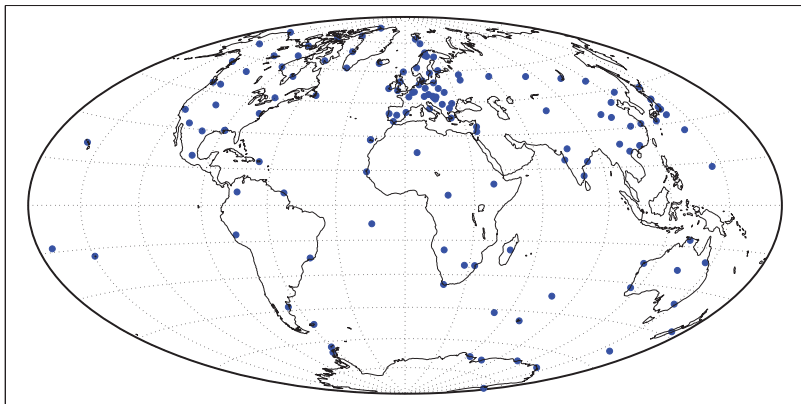


Fig 2.9: Locations of observatories used in determination of recent internal field models.

An obsy series: 1st dif. annual means from ESK

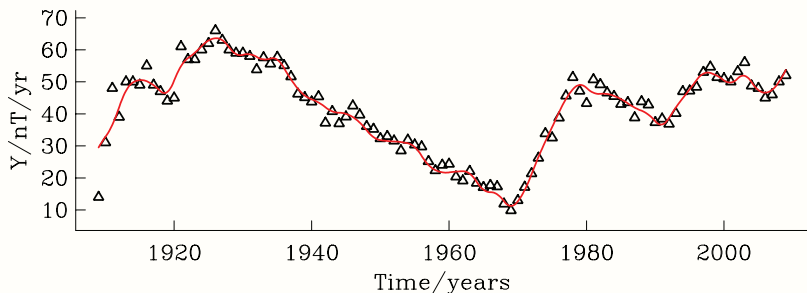


Fig 2.10: First differences of annual means for Eskdalemuir observatory, Scotland. This is a particularly long and high quality record.

- Note the sharp changes in slope of dY/dt (i.e. discontinuity in second time derivative) known as 'jerks'.

Low Earth orbit satellites

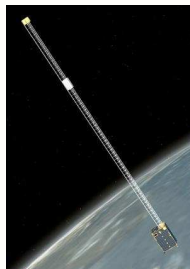


Fig 2.11: Satellites CHAMP (left) and Ørsted (right) measuring the geomagnetic field.

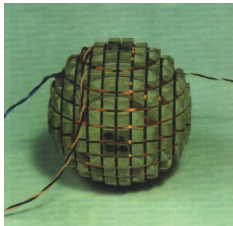


Fig 2.12: Examples of a satellite fluxgate magnetometer (left) and star cameras (right) for measuring instrument orientation.

Geographical coverage with 3 days of satellite data

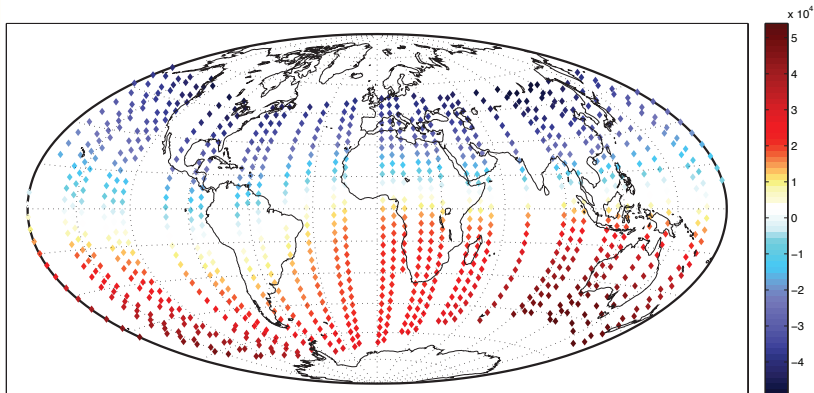


Fig 2.13: Example showing 3 days of CHAMP vector satellite data from 2009 as used in the construction of the CHAOS-4a model of [Olsen et al. \(2012\)](#).

Talk Outline

1. Introduction: The geomagnetic field and the core
2. Sources of magnetic field observations
- 3. Observation-based models of the core field and flow**
4. The Holocene: past 10,000 yrs
5. The recent satellite era: past 13 yrs
6. Handling observational uncertainty: model covariances
7. Outlook

Constructing global models of core surface field

- Model core field as potential field with purely internal source,

$$\mathbf{B} = -\nabla V \quad \text{and} \quad \nabla \cdot \mathbf{B} = 0$$

where
$$V(r, \theta, \phi, t) = a \sum_{n=1}^N \sum_{m=0}^n \left(\frac{a}{r}\right)^{n+1} g_n^m(t) Y_n^m(\theta, \phi).$$

Constructing global models of core surface field

- Model core field as potential field with purely internal source,

$$\mathbf{B} = -\nabla V \quad \text{and} \quad \nabla \cdot \mathbf{B} = 0$$

where
$$V(r, \theta, \phi, t) = a \sum_{n=1}^N \sum_{m=0}^n \left(\frac{a}{r}\right)^{n+1} g_n^m(t) Y_n^m(\theta, \phi).$$

- Account for secular variation using a B-spline basis for Gauss coefficients,

$$g_n^m(t) = \sum_p g_n^{mp} M_p(t).$$

Constructing global models of core surface field

- Model core field as potential field with purely internal source,

$$\mathbf{B} = -\nabla V \quad \text{and} \quad \nabla \cdot \mathbf{B} = 0$$

$$\text{where } V(r, \theta, \phi, t) = a \sum_{n=1}^N \sum_{m=0}^n \left(\frac{a}{r}\right)^{n+1} g_n^m(t) Y_n^m(\theta, \phi).$$

- Account for secular variation using a B-spline basis for Gauss coefficients,

$$g_n^m(t) = \sum_p g_n^{mp} M_p(t).$$

- Solve inverse problem by minimizing a cost function: data misfit & a regularization norm based on core surface field,

$$\Theta = [\mathbf{d} - \mathbf{f}(\mathbf{m})]^T \mathbf{C}_e^{-1} [\mathbf{d} - \mathbf{f}(\mathbf{m})] + \mathcal{R}(\mathbf{m}).$$

$\mathcal{R}(\mathbf{m})$ is a norm measuring spatial & temporal complexity at CMB.

Evolution of radial field at the core surface

Fig 3.1: B_r at core surface, 1590.0-1990.0, *gufm1* ([Jackson et al., 2000](#)): units μT

Evolution of radial field at the core surface

Fig 3.1: B_r at core surface, 1590.0-1990.0, *gufm1* (*Jackson et al., 2000*): units μT

- - High-latitude flux concentrations.
- Reversed field features at mid-latitudes under South Atlantic.
- Series of intense, westward moving, features at low latitude.

Characterising the observed core surface field

Characterising the observed core surface field

- **Spatial properties:**

Characterising the observed core surface field

- **Spatial properties:**
 - Dipole magnitude and direction

Characterising the observed core surface field

- **Spatial properties:**

- Dipole magnitude and direction
- Hemispheric asymmetry (eccentric dipole).
e.g. [Gallet et al. \(2009\)](#), [Olson & Deguen \(2012\)](#)

Characterising the observed core surface field

- **Spatial properties:**
 - Dipole magnitude and direction
 - Hemispheric asymmetry (eccentric dipole).
e.g. [Gallet et al. \(2009\)](#), [Olson & Deguen \(2012\)](#)
 - Spherical harmonic spectra, ratio of dipole to non-dipole power.
e.g. [Loves \(1974\)](#), [Kono & Roberts \(2002\)](#), [Christensen et al. \(2010\)](#)

Characterising the observed core surface field

- **Spatial properties:**

- Dipole magnitude and direction
- Hemispheric asymmetry (eccentric dipole).
e.g. [Gallet et al. \(2009\)](#), [Olson & Deguen \(2012\)](#)
- Spherical harmonic spectra, ratio of dipole to non-dipole power.
e.g. [Loves \(1974\)](#), [Kono & Roberts \(2002\)](#), [Christensen et al. \(2010\)](#)
- Field symmetry, for example ratio of E^S vs E^A .
e.g. [Zhang & Gubbins \(1993\)](#), [Christensen et al. \(2010\)](#)

Characterising the observed core surface field

- **Spatial properties:**

- Dipole magnitude and direction
- Hemispheric asymmetry (eccentric dipole).
e.g. [Gallet et al. \(2009\)](#), [Olson & Deguen \(2012\)](#)
- Spherical harmonic spectra, ratio of dipole to non-dipole power.
e.g. [Lowes \(1974\)](#), [Kono & Roberts \(2002\)](#), [Christensen et al. \(2010\)](#)
- Field symmetry, for example ratio of E^S vs E^A .
e.g. [Zhang & Gubbins \(1993\)](#), [Christensen et al. \(2010\)](#)
- Preferred location of flux patches, dominant waveno., symmetry.
e.g. [Bloxham et al. \(1989\)](#), [Jackson \(2003\)](#), [Gubbins et al. \(2007\)](#)

Characterising the observed core surface field

- **Spatial properties:**

- Dipole magnitude and direction
- Hemispheric asymmetry (eccentric dipole).
e.g. [Gallet et al. \(2009\)](#), [Olson & Deguen \(2012\)](#)
- Spherical harmonic spectra, ratio of dipole to non-dipole power.
e.g. [Lowes \(1974\)](#), [Kono & Roberts \(2002\)](#), [Christensen et al. \(2010\)](#)
- Field symmetry, for example ratio of E^S vs E^A .
e.g. [Zhang & Gubbins \(1993\)](#), [Christensen et al. \(2010\)](#)
- Preferred location of flux patches, dominant waveno., symmetry.
e.g. [Bloxham et al. \(1989\)](#), [Jackson \(2003\)](#), [Gubbins et al. \(2007\)](#)

- **Temporal properties:**

Characterising the observed core surface field

- **Spatial properties:**

- Dipole magnitude and direction
- Hemispheric asymmetry (eccentric dipole).
e.g. Gallet et al. (2009), Olson & Deguen (2012)
- Spherical harmonic spectra, ratio of dipole to non-dipole power.
e.g. Lowes (1974), Kono & Roberts (2002), Christensen et al. (2010)
- Field symmetry, for example ratio of E^S vs E^A .
e.g. Zhang & Gubbins (1993), Christensen et al. (2010)
- Preferred location of flux patches, dominant waveno., symmetry.
e.g. Bloxham et al. (1989), Jackson (2003), Gubbins et al. (2007)

- **Temporal properties:**

- Temporal power spectra including fluctuations in dipole.
e.g. Constable & Johnson (2005), Olson et al. (2012)

Characterising the observed core surface field

- **Spatial properties:**

- Dipole magnitude and direction
- Hemispheric asymmetry (eccentric dipole).
e.g. Gallet et al. (2009), Olson & Deguen (2012)
- Spherical harmonic spectra, ratio of dipole to non-dipole power.
e.g. Lowes (1974), Kono & Roberts (2002), Christensen et al. (2010)
- Field symmetry, for example ratio of E^S vs E^A .
e.g. Zhang & Gubbins (1993), Christensen et al. (2010)
- Preferred location of flux patches, dominant waveno., symmetry.
e.g. Bloxham et al. (1989), Jackson (2003), Gubbins et al. (2007)

- **Temporal properties:**

- Temporal power spectra including fluctuations in dipole.
e.g. Constable & Johnson (2005), Olson et al. (2012)
- Timescale as a function of spherical harmonic degree.
e.g. Hulot & LeMouél (1994), Holme & Olsen (2006), Christensen et al. (2012)

Characterising the observed core surface field

- **Spatial properties:**

- Dipole magnitude and direction
- Hemispheric asymmetry (eccentric dipole).
e.g. Gallet et al. (2009), Olson & Deguen (2012)
- Spherical harmonic spectra, ratio of dipole to non-dipole power.
e.g. Lowes (1974), Kono & Roberts (2002), Christensen et al. (2010)
- Field symmetry, for example ratio of E^S vs E^A .
e.g. Zhang & Gubbins (1993), Christensen et al. (2010)
- Preferred location of flux patches, dominant waveno., symmetry.
e.g. Bloxham et al. (1989), Jackson (2003), Gubbins et al. (2007)

- **Temporal properties:**

- Temporal power spectra including fluctuations in dipole.
e.g. Constable & Johnson (2005), Olson et al. (2012)
- Timescale as a function of spherical harmonic degree.
e.g. Hulot & LeMouél (1994), Holme & Olsen (2006), Christensen et al. (2012)
- Motions of flux patches: Azimuthal & meridional motions.
e.g. Finlay & Jackson (2003), Amit et al. (2011)

Characterising the observed core surface field

● Spatial properties:

- Dipole magnitude and direction
- Hemispheric asymmetry (eccentric dipole).
e.g. Gallet et al. (2009), Olson & Deguen (2012)
- Spherical harmonic spectra, ratio of dipole to non-dipole power.
e.g. Lowes (1974), Kono & Roberts (2002), Christensen et al. (2010)
- Field symmetry, for example ratio of E^S vs E^A .
e.g. Zhang & Gubbins (1993), Christensen et al. (2010)
- Preferred location of flux patches, dominant waveno., symmetry.
e.g. Bloxham et al. (1989), Jackson (2003), Gubbins et al. (2007)

● Temporal properties:

- Temporal power spectra including fluctuations in dipole.
e.g. Constable & Johnson (2005), Olson et al. (2012)
- Timescale as a function of spherical harmonic degree.
e.g. Hulot & LeMouél (1994), Holme & Olsen (2006), Christensen et al. (2012)
- Motions of flux patches: Azimuthal & meridional motions.
e.g. Finlay & Jackson (2003), Amit et al. (2011)
- Flux emergence.
e.g. Gubbins (1996), Chulliat & Olsen (2010)

Characterising the observed core surface field

• Spatial properties:

- Dipole magnitude and direction
- Hemispheric asymmetry (eccentric dipole).
e.g. Gallet et al. (2009), Olson & Deguen (2012)
- Spherical harmonic spectra, ratio of dipole to non-dipole power.
e.g. Lowes (1974), Kono & Roberts (2002), Christensen et al. (2010)
- Field symmetry, for example ratio of E^S vs E^A .
e.g. Zhang & Gubbins (1993), Christensen et al. (2010)
- Preferred location of flux patches, dominant waveno., symmetry.
e.g. Bloxham et al. (1989), Jackson (2003), Gubbins et al. (2007)

• Temporal properties:

- Temporal power spectra including fluctuations in dipole.
e.g. Constable & Johnson (2005), Olson et al. (2012)
- Timescale as a function of spherical harmonic degree.
e.g. Hulot & LeMouél (1994), Holme & Olsen (2006), Christensen et al. (2012)
- Motions of flux patches: Azimuthal & meridional motions.
e.g. Finlay & Jackson (2003), Amit et al. (2011)
- Flux emergence.
e.g. Gubbins (1996), Chulliat & Olsen (2010)

- Ultimate criteria: full space-time description & covariance estimates

Induction Eqn: linking field change and core flow

- Under the MHD approximation, Maxwell's equations reduce to:

$$\frac{\partial \mathbf{B}}{\partial t} = \nabla \times (\mathbf{u} \times \mathbf{B}) + \eta \nabla^2 \mathbf{B}$$

Induction Eqn: linking field change and core flow

- Under the MHD approximation, Maxwell's equations reduce to:

$$\frac{\partial \mathbf{B}}{\partial t} = \nabla \times (\mathbf{u} \times \mathbf{B}) + \eta \nabla^2 \mathbf{B}$$

- Assuming incompressible flow, at the core surface where $u_r=0$:

$$\frac{\partial B_r}{\partial t} + \mathbf{u}_H \cdot \nabla_H B_r + B_r (\nabla_H \cdot \mathbf{u}_H) = \eta \left[\frac{1}{r^2} \frac{\partial^2}{\partial r^2} (r^2 B_r) + \nabla_H^2 B_r \right]$$

where $\nabla_H = \nabla - (\partial/\partial r)\hat{\mathbf{r}}$ and $\eta = 1/\sigma\mu_0$ is the magnetic diffusivity.

Induction Eqn: linking field change and core flow

- Under the MHD approximation, Maxwell's equations reduce to:

$$\frac{\partial \mathbf{B}}{\partial t} = \nabla \times (\mathbf{u} \times \mathbf{B}) + \eta \nabla^2 \mathbf{B}$$

- Assuming incompressible flow, at the core surface where $u_r=0$:

$$\frac{\partial B_r}{\partial t} + \mathbf{u}_H \cdot \nabla_H B_r + B_r (\nabla_H \cdot \mathbf{u}_H) = \eta \left[\frac{1}{r^2} \frac{\partial^2}{\partial r^2} (r^2 B_r) + \nabla_H^2 B_r \right]$$

where $\nabla_H = \nabla - (\partial/\partial r)\hat{\mathbf{r}}$ and $\eta = 1/\sigma\mu_0$ is the magnetic diffusivity.

- Further neglecting magnetic diffusion then

$$\frac{\partial B_r}{\partial t} + \mathbf{u}_H \cdot \nabla_H B_r + B_r (\nabla_H \cdot \mathbf{u}_H) = 0$$

Induction Eqn: linking field change and core flow

- Under the MHD approximation, Maxwell's equations reduce to:

$$\frac{\partial \mathbf{B}}{\partial t} = \nabla \times (\mathbf{u} \times \mathbf{B}) + \eta \nabla^2 \mathbf{B}$$

- Assuming incompressible flow, at the core surface where $u_r=0$:

$$\frac{\partial B_r}{\partial t} + \mathbf{u}_H \cdot \nabla_H B_r + B_r (\nabla_H \cdot \mathbf{u}_H) = \eta \left[\frac{1}{r^2} \frac{\partial^2}{\partial r^2} (r^2 B_r) + \nabla_H^2 B_r \right]$$

where $\nabla_H = \nabla - (\partial/\partial r)\hat{\mathbf{r}}$ and $\eta = 1/\sigma\mu_0$ is the magnetic diffusivity.

- Further neglecting magnetic diffusion then

$$\frac{\partial B_r}{\partial t} + \mathbf{u}_H \cdot \nabla_H B_r + B_r (\nabla_H \cdot \mathbf{u}_H) = 0$$

- In this case, field evolves via a "frozen flux" mechanism (see [Gubbins \(1996\)](#) or [Amit & Christensen \(2008\)](#) for other approaches)

Inversion for core flow

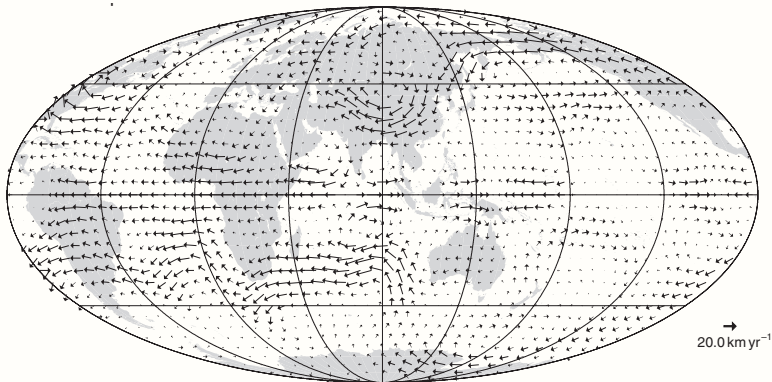


Fig 3.2: Example tangentially geostrophic core flow (Holme & Olsen, 2006) that accounts for much of the observed field change.

Fit to changes in the length of day

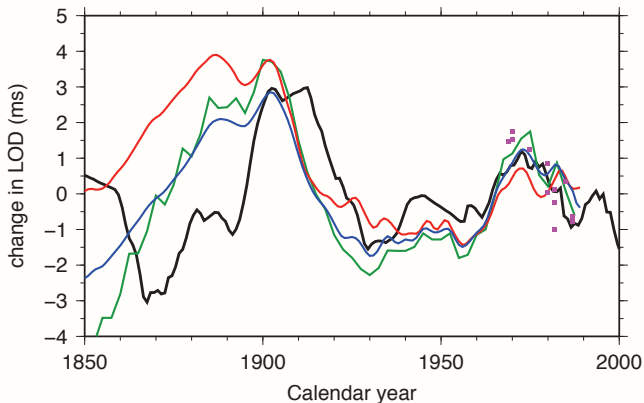


Fig 3.3: Observed changes in LOD (black line) versus predictions from purple squares = Jault et al. (1988); blue = Jackson (1997); green = Hide (2000); red = Pais & Hulot (2000), courtesy of M. Dumberry.

- Uses time variations of the equatorially symmetric, zonal flows, extended rigidly inside the core.

Stronger assumption: Quasi-geostrophic flow

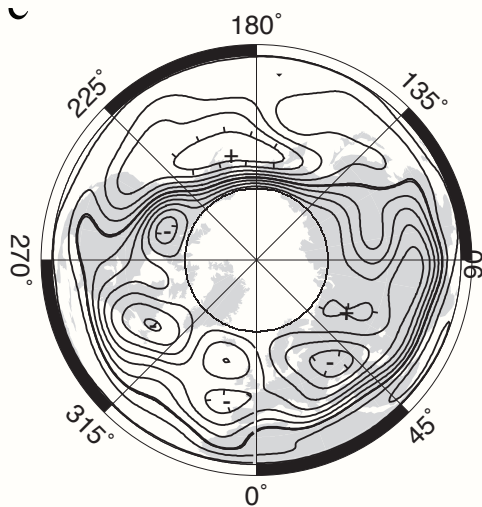


Fig 3.4: Example quasi-geostrophic core flow derived using the method of [Gillet et al. \(2009\)](#), courtesy of A. Pais.

Talk Outline

1. Introduction: The geomagnetic field and the core
2. Sources of magnetic field observations
3. Observation-based models of the core field and flow
- 4. The Holocene: past 10,000 yrs**
5. The recent satellite era: past 13 yrs
6. Handling observational uncertainty: model covariances
7. Outlook

Fit to lake sediment data

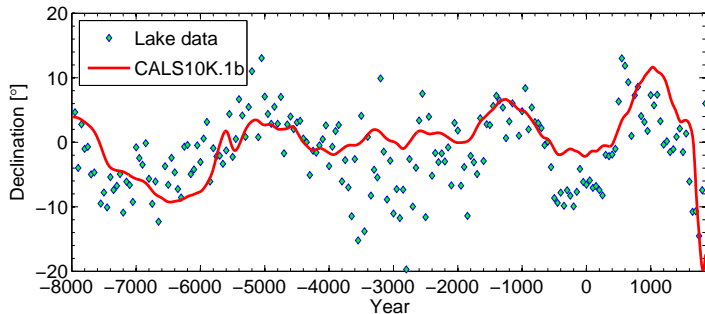


Fig 4.1: Example of fit of CALS10k.1b model (Korte et al., 2011) to declination D from the Eifel Maar record, Germany.

- Model fits long term trends and most persistent features across sediment records.

Time-averaged field, past 10 kyrs

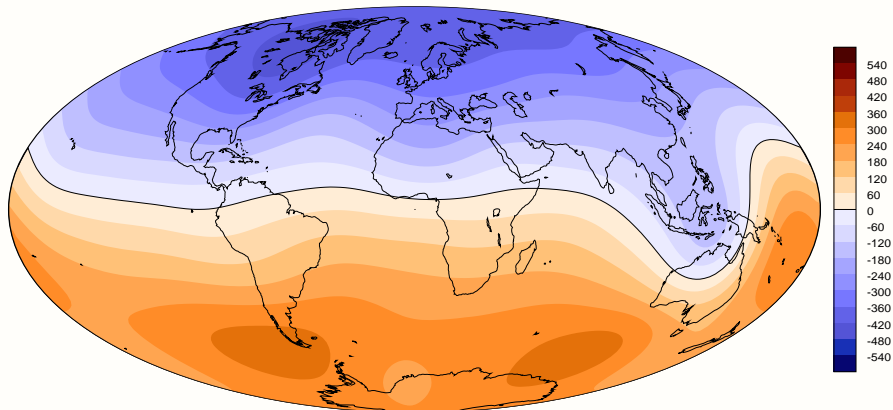


Fig 4.3: Radial field at CMB averaged over 8000BC to 1500AD, CALS10k.1 (Korte et al., 2011).

- Evidence for persistent non-axisymmetric structure over 10 kyrs.
- Supports hypothesis that CMB heat flow pattern affects geodynamo.

Dipole moment variation

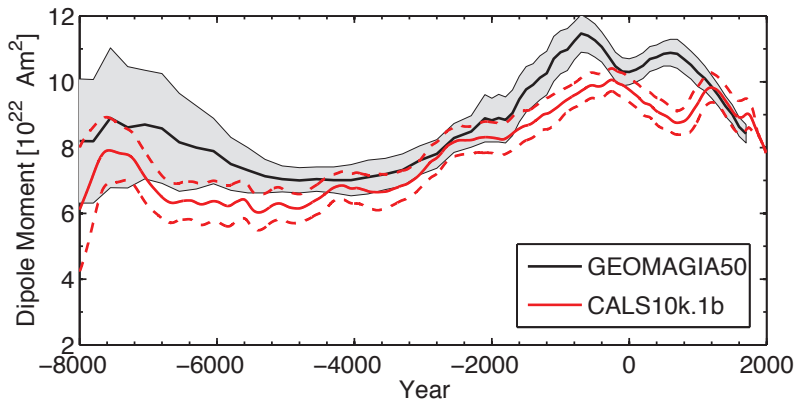


Fig 4.4: Comparison of dipole moment inferred from the GEOMAGIA-50 database (Donadini et al., 2006) using a VDM approach and that inferred from the CALS10k.1 model (Korte et al., 2011).

- Dipole moment increased from $\sim 5000\text{BC}$ to $\sim 500\text{BC}$.
- Has been decaying since that time, but not monotonically.

Talk Outline

1. Introduction: The geomagnetic field and the core
2. Sources of magnetic field observations
3. Observation-based models of the core field and flow
4. The Holocene: past 10,000 yrs
- 5. The recent satellite era: past 13 yrs**
6. Handling observational uncertainty: model covariances
7. Outlook

Fit to observatory data: dZ/dt at HER

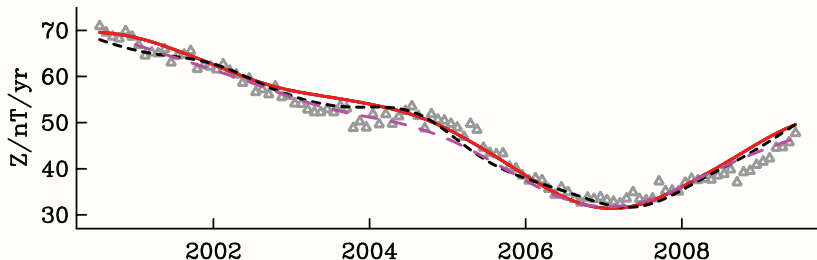


Fig 5.1 : Comparison of observed and modelled rate of change of Z field components at Hermanus, South Africa. Observations are annual differences of month means (grey triangles). Red solid line is *gufm-sat-E3* (Finlay et al., 2012), black dashed line is *CHAOS-3* (Olsen et al., 2010) and pink dashed line is *GRIMM-2* (Lesur et al., 2010).

Core surface radial field in 2005

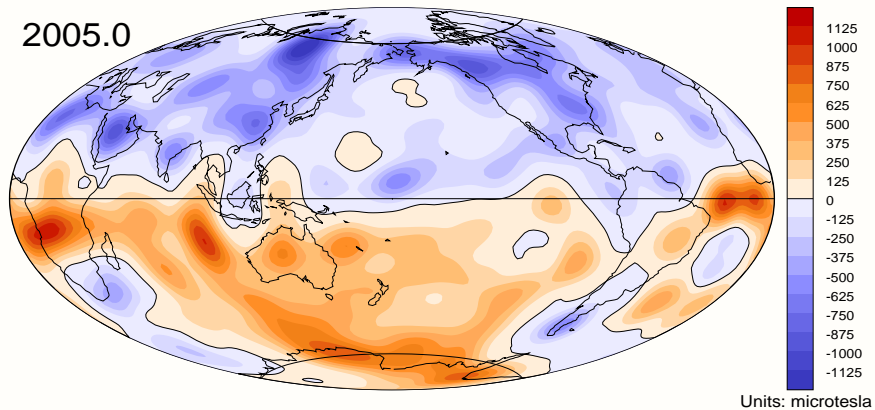


Fig 5.2: Radial component of field at core surface in 2005 from *gufm-sat-E3* (Finlay et al., 2012).

- High latitude patches involve several sub-structures
- Flux spot under eastern Indian ocean has intensified in past 20 years.

Core surface radial field: secular variation in 2005

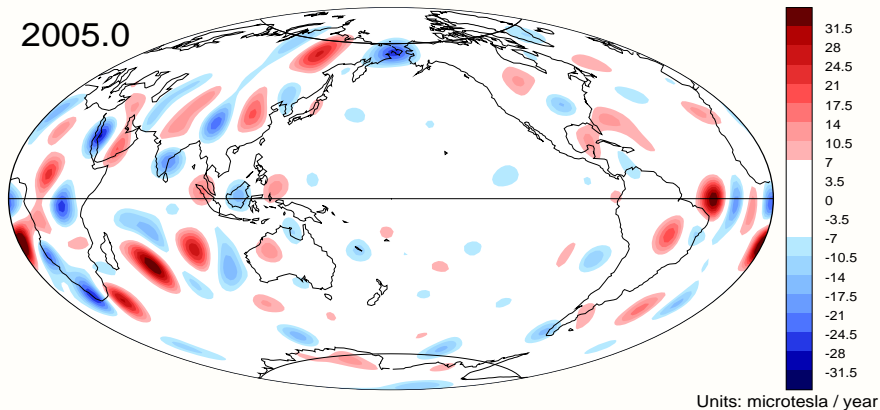


Fig 5.3: Radial component of SV at core surface in 2005 from *gufm-sat-E3* (Finlay et al., 2012).

- Low amplitude field change under the Pacific (Holme et al., 2011).
- Most vigorous changes occur outside the tangent cylinder.

Core surface radial field: secular acceln. in 2005

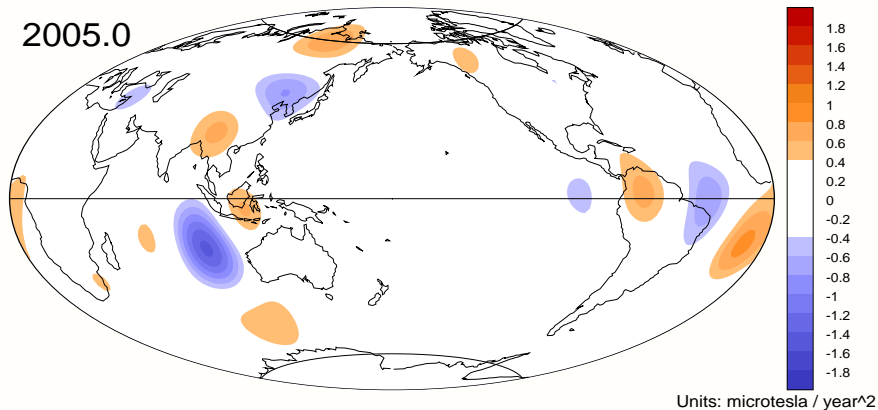


Fig 5.4: Radial component of SA at core surface in 2005 from *gufm-sat-E3* (Finlay et al., 2012).

- Localized pulse of acceleration under eastern Indian ocean in 2006.
- Most rapid changes generally occur at low latitudes.

Global timescales for field change

- Ratio of MF and SV power spectra yields a timescale for the field to entirely change as a function of SH degree ([Hulot & LeMouél, 1994](#)).

$$\tau_g(n) = \sqrt{\frac{\sum_{m=0}^n [(g_n^m)^2 + (h_n^m)^2]}{\sum_{m=0}^n [(\dot{g}_n^m)^2 + (\dot{h}_n^m)^2]}} \quad \text{MF timescale}$$

Global timescales for field change

- Ratio of MF and SV power spectra yields a timescale for the field to entirely change as a function of SH degree (Hulot & LeMouél, 1994).

$$\tau_g(n) = \sqrt{\frac{\sum_{m=0}^n [(g_n^m)^2 + (h_n^m)^2]}{\sum_{m=0}^n [\dot{g}_n^m)^2 + (\dot{h}_n^m)^2]}} \quad \text{MF timescale}$$

- One can define a similar timescale on which the secular variation completely changes (Holme et al., 2011)

$$\tau_{\dot{g}}(n) = \sqrt{\frac{\sum_{m=0}^n [(\dot{g}_n^m)^2 + (\dot{h}_n^m)^2]}{\sum_{m=0}^n [(\ddot{g}_n^m)^2 + (\ddot{h}_n^m)^2]}} \quad \text{SV timescale}$$

- May be calculated from time-dependent field models to give a useful global diagnostic of field change.

Timescales from satellite era field model

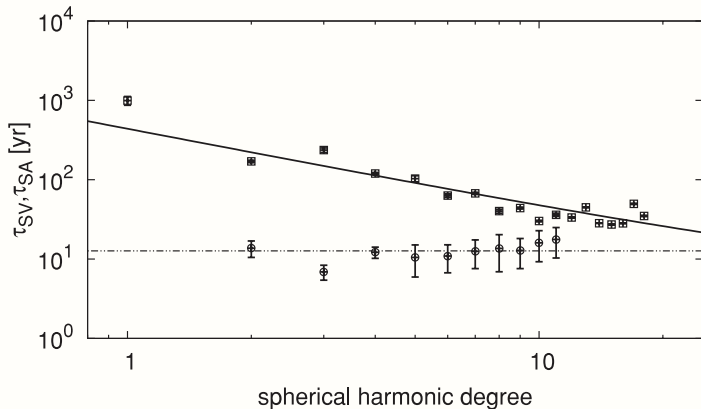


Fig 5.5: Timescales as a function of degree, from the GRIMM-3 model (Christensen et al., 2012).

- As pointed out by Holme et al. (2011) an approximately constant timescale of 10 years is obtained for $\tau_{\dot{g}}(n)$ in present field models.

Timescales from dynamo simulations

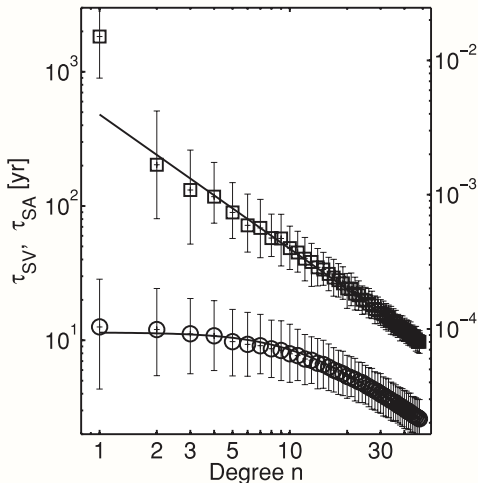


Fig 5.6: Timescale as a function of degree from a dynamo simulation (Christensen et al., 2012).

- Rescaling dynamo time to the Earth a similar timescale of 10 yrs can be obtained for low degrees, provided $Rm \sim 1000$.

A cautionary note: timescales and regularization

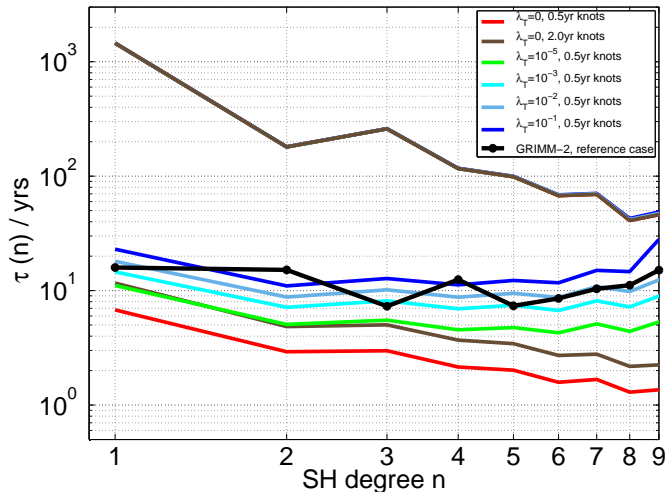


Fig 5.7: Test using perfect coverage of noise-free Z observations at 350km sampled every 0.2yrs: input allows rapid changes - colours show inversions with different knot spacings and damping parameters.

Remarks on field evolution in the satellite era

Remarks on field evolution in the satellite era

- SA occurs in short-lived, localized bursts (Olsen & Manda, 2008; Lesur et al., 2008), most notably at low latitudes.
- Pacific hemisphere has weaker field and lower SV and SA (Holme et al., 2011; Finlay et al., 2012).

Remarks on field evolution in the satellite era

- SA occurs in short-lived, localized bursts (Olsen & Manda, 2008; Lesur et al., 2008), most notably at low latitudes.
- Pacific hemisphere has weaker field and lower SV and SA (Holme et al., 2011; Finlay et al., 2012).
- Silva & Hulot (2012) showed zonal flow accel. is insufficient to account for field evolution in 2003, in contrast to more general QG flows permitting changes in the (equatorially symmetric) meridional flow.
- Schaeffer & Pais (2011) suggest permitting stronger (anisotropic) zonal flows helps improve fit to changes in the LOD.

Remarks on field evolution in the satellite era

- SA occurs in short-lived, localized bursts (Olsen & Manda, 2008; Lesur et al., 2008), most notably at low latitudes.
- Pacific hemisphere has weaker field and lower SV and SA (Holme et al., 2011; Finlay et al., 2012).
- Silva & Hulot (2012) showed zonal flow accel. is insufficient to account for field evolution in 2003, in contrast to more general QG flows permitting changes in the (equatorially symmetric) meridional flow.
- Schaeffer & Pais (2011) suggest permitting stronger (anisotropic) zonal flows helps improve fit to changes in the LOD.
- Temporal smoothing applied in current field models may filter out rapid, but physically interesting signals.

Talk Outline

1. Introduction: The geomagnetic field and the core
2. Sources of magnetic field observations
3. Observation-based models of the core field and flow
4. The Holocene: past 10,000 yrs
5. The recent satellite era: past 13 yrs
- 6. Handling observational uncertainty: model covariances**
7. Outlook

Probabilistic (Bayesian) approach to field modelling

- Recall the geomagnetic forward problem: $\mathbf{d} = f(\mathbf{m}) + \mathbf{e}$
Statistics of \mathbf{e} described by \mathbf{C}_e . Prior knowledge on \mathbf{m} by \mathbf{C}_m .

Probabilistic (Bayesian) approach to field modelling

- Recall the geomagnetic forward problem: $\mathbf{d} = f(\mathbf{m}) + \mathbf{e}$
Statistics of \mathbf{e} described by \mathbf{C}_e . Prior knowledge on \mathbf{m} by \mathbf{C}_m .
- Bayesian soln: **posterior pdf**, given prior knowledge & observations.

Probabilistic (Bayesian) approach to field modelling

- Recall the geomagnetic forward problem: $\mathbf{d} = \mathbf{f}(\mathbf{m}) + \mathbf{e}$
Statistics of \mathbf{e} described by \mathbf{C}_e . Prior knowledge on \mathbf{m} by \mathbf{C}_m .
- Bayesian soln: **posterior pdf**, given prior knowledge & observations.
- Gaussian statistics: find the model $\bar{\mathbf{m}}$ with maximum posterior prob also spread of posterior pdf by minimizing cost fn:

$$\Theta = [\mathbf{d} - \mathbf{f}(\mathbf{m})]^T \mathbf{C}_e^{-1} [\mathbf{d} - \mathbf{f}(\mathbf{m})] + \mathbf{m}^T \mathbf{C}_m^{-1} \mathbf{m}$$

Probabilistic (Bayesian) approach to field modelling

- Recall the geomagnetic forward problem: $\mathbf{d} = \mathbf{f}(\mathbf{m}) + \mathbf{e}$
Statistics of \mathbf{e} described by \mathbf{C}_e . Prior knowledge on \mathbf{m} by \mathbf{C}_m .
- Bayesian soln: **posterior pdf**, given prior knowledge & observations.
- Gaussian statistics: find the model $\bar{\mathbf{m}}$ with maximum posterior prob also spread of posterior pdf by minimizing cost fn:

$$\Theta = [\mathbf{d} - \mathbf{f}(\mathbf{m})]^T \mathbf{C}_e^{-1} [\mathbf{d} - \mathbf{f}(\mathbf{m})] + \mathbf{m}^T \mathbf{C}_m^{-1} \mathbf{m}$$

- Do this using an iterative Newton-type algorithm

$$\mathbf{m}_{i+1} = \mathbf{m}_i + \mathbf{C} \{ \nabla f(\mathbf{m}_i) \mathbf{C}_e^{-1} [\mathbf{d} - \mathbf{f}(\mathbf{m}_i)] - \mathbf{C}_m^{-1} \mathbf{m}_i \}$$

$$\text{where } \mathbf{C} = [\nabla f(\mathbf{m}_i)^T \mathbf{C}_e^{-1} \nabla f(\mathbf{m}_i) + \mathbf{C}_m^{-1}]^{-1}$$

Probabilistic (Bayesian) approach to field modelling

- Recall the geomagnetic forward problem: $\mathbf{d} = f(\mathbf{m}) + \mathbf{e}$
Statistics of \mathbf{e} described by \mathbf{C}_e . Prior knowledge on \mathbf{m} by \mathbf{C}_m .
- Bayesian soln: **posterior pdf**, given prior knowledge & observations.
- Gaussian statistics: find the model $\bar{\mathbf{m}}$ with maximum posterior prob also spread of posterior pdf by minimizing cost fn:

$$\Theta = [\mathbf{d} - \mathbf{f}(\mathbf{m})]^T \mathbf{C}_e^{-1} [\mathbf{d} - \mathbf{f}(\mathbf{m})] + \mathbf{m}^T \mathbf{C}_m^{-1} \mathbf{m}$$

- Do this using an iterative Newton-type algorithm

$$\mathbf{m}_{i+1} = \mathbf{m}_i + \mathbf{C} \{ \nabla f(\mathbf{m}_i) \mathbf{C}_e^{-1} [\mathbf{d} - \mathbf{f}(\mathbf{m}_i)] - \mathbf{C}_m^{-1} \mathbf{m}_i \}$$

$$\text{where } \mathbf{C} = [\nabla f(\mathbf{m}_i)^T \mathbf{C}_e^{-1} \nabla f(\mathbf{m}_i) + \mathbf{C}_m^{-1}]^{-1}$$

- **Sample posterior pdf** (defined by both $\bar{\mathbf{m}}$ and \mathbf{C}) to generate an **ensemble of models** characterising the solution.
- When no obs, ensemble has statistics specified by prior \mathbf{C}_m .

Stochastic process prior for field modelling

Stochastic process prior for field modelling

- Assume **zero mean, stationary, random process**.
- No covariance between coeffs and identical covariance sequences for coeffs with same degree.

$$C_n(\tau) = \sigma_n^2 \rho_n(\tau)$$

Stochastic process prior for field modelling

- Assume **zero mean, stationary, random process**.
- No covariance between coeffs and identical covariance sequences for coeffs with same degree.

$$C_n(\tau) = \sigma_n^2 \rho_n(\tau)$$

- Set prior variances σ_n^2 according to satellite field models.
- Our prior on correlation: $\rho_n(\tau)$ is that of an AR(2) process:

$$\rho_n(\tau) = \left[1 + \sqrt{3} \frac{|\tau|}{\tau_c} \right] \exp \left(-\frac{\sqrt{3}|\tau|}{\tau_c} \right)$$

Intrinsic timescale τ_c based on τ_g from satellite field models.

Stochastic process prior for field modelling

- Assume **zero mean, stationary, random process**.
- No covariance between coeffs and identical covariance sequences for coeffs with same degree.

$$C_n(\tau) = \sigma_n^2 \rho_n(\tau)$$

- Set prior variances σ_n^2 according to satellite field models.
- Our prior on correlation: $\rho_n(\tau)$ is that of an AR(2) process:

$$\rho_n(\tau) = \left[1 + \sqrt{3} \frac{|\tau|}{\tau_c} \right] \exp \left(-\frac{\sqrt{3}|\tau|}{\tau_c} \right)$$

Intrinsic timescale τ_c based on τ_g from satellite field models.

- Allows discontinuities in d^2B/dt^2 ('jerks') & spectral slope f^{-4} .

Stochastic process prior for field modelling

- Assume **zero mean, stationary, random process**.
- No covariance between coeffs and identical covariance sequences for coeffs with same degree.

$$C_n(\tau) = \sigma_n^2 \rho_n(\tau)$$

- Set prior variances σ_n^2 according to satellite field models.
- Our prior on correlation: $\rho_n(\tau)$ is that of an AR(2) process:

$$\rho_n(\tau) = \left[1 + \sqrt{3} \frac{|\tau|}{\tau_c} \right] \exp \left(-\frac{\sqrt{3}|\tau|}{\tau_c} \right)$$

Intrinsic timescale τ_c based on τ_g from satellite field models.

- Allows discontinuities in d^2B/dt^2 ('jerks') & spectral slope f^{-4} .
- Algorithm familiar except **C_m is dense** and **no damping parameter**.

Fit of ensemble of model to obsy annual means

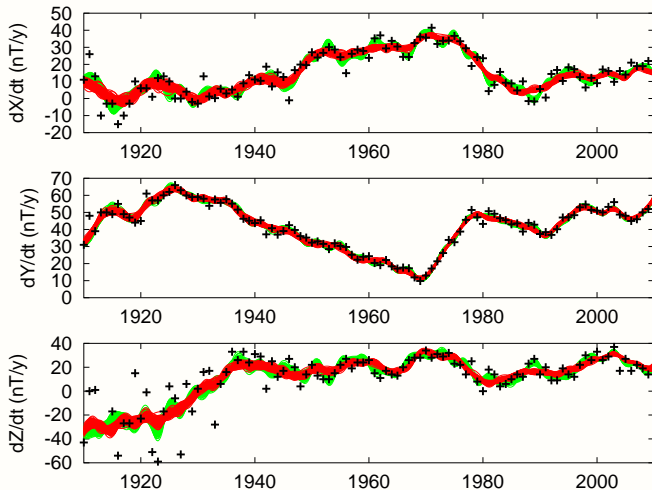


Fig 6.1: Fit of ensemble of COV-OBS field models (Gillet et al., in prep) to observatory annual means from Eskdalemuir (UK). Red are internal field models only, green includes ext. dipole.

Secular variation of axial dipole

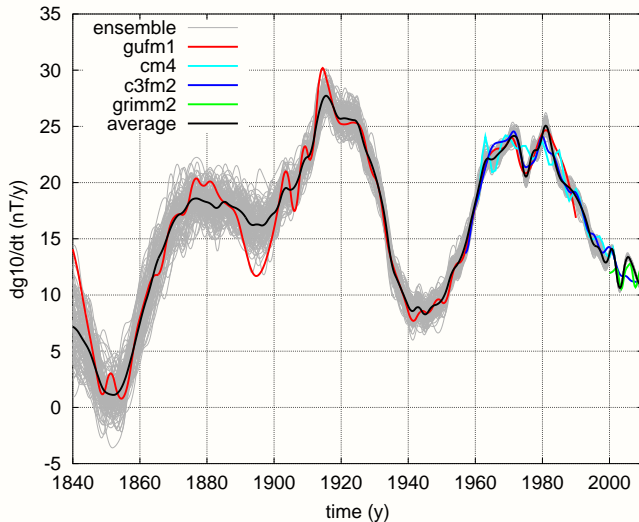


Fig 6.2: Evolution of axial dipole $g_1^0(t)$ in COV-OBS models of (Gillet et al., in prep).

Secular variation of higher sectorial coefficient

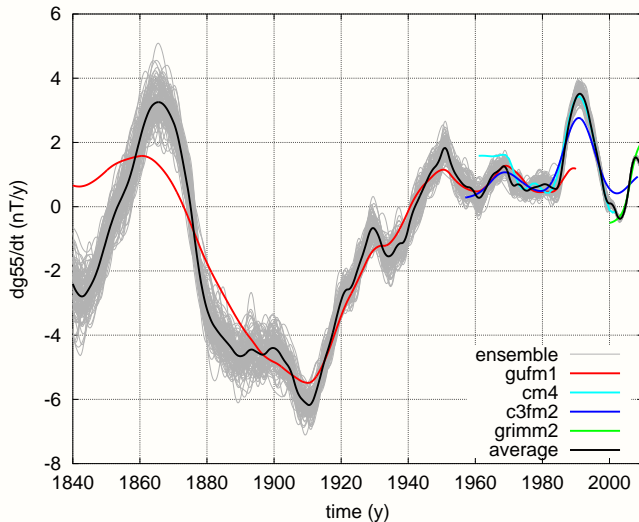


Fig 6.3: Time evolution of the $g_5^5(t)$ sectorial coefficient in COV-OBS models (Gillet et al., in prep).

Realizations of core surface field in 1920

Fig 6.4: B_r at core surface in 1920.0 from the *COV-OBS* model (Gillet *et al.*, *in prep*) : units μT

- Some features are persistently present, others not.

Model covariance matrix at one epoch

- Solution characterized not only by $\bar{\mathbf{m}}$ but also by \mathbf{C}
- \mathbf{C} encapsulates model uncertainties and their correlations btw coeff.

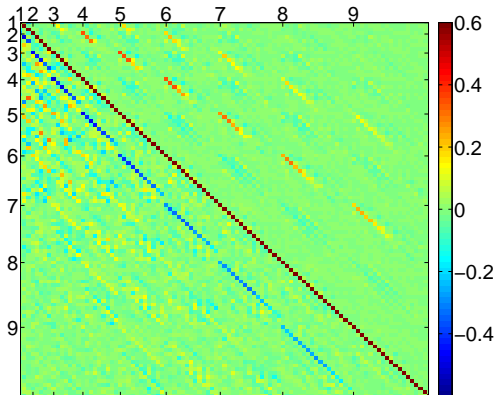


Fig 6.5: Model covariance matrix in 1925 (bottom) and 2005 (top) from COV-OBS model (Gillet et al., in prep).

Other recent methodological developments

- Flux constrained modelling techniques - [Wardinski & Lesur \(2012\)](#).

Other recent methodological developments

- Flux constrained modelling techniques - [Wardinski & Lesur \(2012\)](#).
- Important tools for combining core physics-based numerical models and observation-based field models have been developed:
 - Sequential assimilation e.g. [Kuang et al. \(2009\)](#), [Aubert & Fournier \(2011\)](#).
 - Variational assimilation e.g. [Canet et al. \(2009\)](#); [Li et al. \(2011\)](#).

Talk Outline

1. Introduction: The geomagnetic field and the core
2. Sources of magnetic field observations
3. Observation-based models of the core field and flow
4. The Holocene: past 10,000 yrs
5. The recent satellite era: past 13 yrs
6. Handling observational uncertainty: model covariances
- 7. Outlook**

Swarm: A new satellite constellation

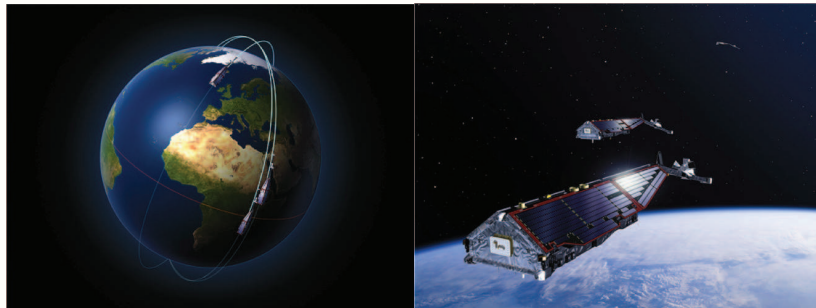


Fig 7.1: Artist's visualization of Swarm satellites due for launch in late 2012. Credit: ESA

- ESA's SWARM mission (due for launch this year) should provide further high quality global observations in the upcoming years.
- Three satellites flying at 400 - 550 km altitude.
- Will enable improved characterization of the external field and better knowledge of azimuthal field gradients (Friis-Christensen et al., 2006).
- Aiming at improved resolution of core field time-changes.

Well-dated archeo/paleo-magnetic records



Fig 7.2: Examples of South African potteries for archeomagnetic analysis (Neukirch et al., 2012).

- Ongoing efforts to improve global coverage with well-dated samples.
- Urgently need older archeomag records to supplement RPI.

Detailed comparisons with low E simulations

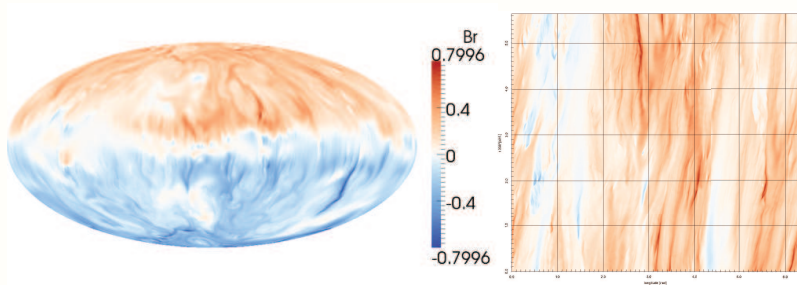


Fig 7.3: Radial magnetic field at the outer boundary and its time evolution at 15 degrees North from a simulation with $E = 10^{-6}$, $q = 0.05$, $Rm = 260$. Courtesy of A. Sheyko.

- Need to undertake detailed comparisons of space-time field evolution patterns and not restrict analysis to simple global measures.
- A major challenge is now to develop schemes whereby observations directly constrain more realistic dynamical models.
- But need to acknowledge both observations and models are imperfect - stochastic element necessary? (talk of N. Gillet)

Conclusions

Conclusions

- Magnetic observations provide information both on the long term evolution and rapid changes taking place in the core.

Conclusions

- Magnetic observations provide information both on the long term evolution and rapid changes taking place in the core.
- Include indirect paleomagnetic records, historical measurements and data collected by ground observatories and satellites.

Conclusions

- Magnetic observations provide information both on the long term evolution and rapid changes taking place in the core.
- Include indirect paleomagnetic records, historical measurements and data collected by ground observatories and satellites.
- Provide spatial & temporal constraints, but time-varying resolution.

Conclusions

- Magnetic observations provide information both on the long term evolution and rapid changes taking place in the core.
- Include indirect paleomagnetic records, historical measurements and data collected by ground observatories and satellites.
- Provide spatial & temporal constraints, but time-varying resolution.
- Field models spanning the past 10kyrs show time-averaged non-axisymmetric structure indicative of CMB (or ICB?) conditions.

Conclusions

- Magnetic observations provide information both on the long term evolution and rapid changes taking place in the core.
- Include indirect paleomagnetic records, historical measurements and data collected by ground observatories and satellites.
- Provide spatial & temporal constraints, but time-varying resolution.
- Field models spanning the past 10kyrs show time-averaged non-axisymmetric structure indicative of CMB (or ICB?) conditions.
- Ten years of satellite observation reveals rapid field change occurs locally in bursts, e.g. low latitudes under the Atlantic.

Conclusions

- Magnetic observations provide information both on the long term evolution and rapid changes taking place in the core.
- Include indirect paleomagnetic records, historical measurements and data collected by ground observatories and satellites.
- Provide spatial & temporal constraints, but time-varying resolution.
- Field models spanning the past 10kyrs show time-averaged non-axisymmetric structure indicative of CMB (or ICB?) conditions.
- Ten years of satellite observation reveals rapid field change occurs locally in bursts, e.g. low latitudes under the Atlantic.
- Beyond simple comparisons, covariances must be propagated when magnetic observations are used to assess models of the deep Earth.

- Amit, H. & Christensen, U., 2008. Accounting for magnetic diffusion in core flow inversions from geomagnetic secular variation, *Geophys. J. Int.*, **175**, 913–924.
- Amit, H., Korte, M., Aubert, J., Constable, C., & Hulot, G., 2011. The time-dependence of intense archeomagnetic flux patches, *J. Geophys. Res.*, **175**, doi:10.1029/2011JB008538.
- Aubert, J. & Fournier, A., 2011. Inferring internal properties of earth's core dynamics and their evolution from surface observations and a numerical geodynamo model, *Non. Proc. Geophys.*, **18**, 657–674.
- Bloxham, J., Gubbins, D., & Jackson, A., 1989. Geomagnetic secular variation, *Phil. Trans. R. Soc. Lond. A*, **329**(1606), 415–502.
- Canet, E., Fournier, A., & Jault, D., 2009. Forward and adjoint quasi-geostrophic models of the geomagnetic secular variation, *J. Geophys. Res.*, p. in prep.
- Christensen, U. R., Aubert, J., & Hulot, G., 2010. Conditions for earth-like geodynamo models, *Earth Planet. Sci. Lett.*, **296**, 487–496.
- Christensen, U. R., Wardinski, I., & Lesur, V., 2012. Timescales of geomagnetic secular acceleration in satellite field models and geodynamo models, *Geophys. J. Int.*, **190**, 243–252.
- Chulliat, A. & Olsen, N., 2010. Observation of magnetic diffusion in the earth's outer core from magSAT, Ørsted, and CHAMP data, *J. Geophys. Res.*, **115**, doi:10.1029/2009JB006994.
- Constable, C. G. & Constable, S., 2004. Satellite magnetic field measurements: applications in studying the deep earth, *In: The State of the Planet: Frontiers and Challenges in Geophysics*, Edited by R.J.S. Sparks and C.J. Hawkesworth, pp. 147–160.
- Constable, C. G. & Johnson, C. L., 2005. A paleomagnetic power spectrum, *Phys. Earth Planet. Int.*, **153**, 61–73.
- Donadini, F., Korhonen, K., Riisager, P., & Pesonen, L., 2006. Database for holocene geomagnetic intensity information, *EOS*, **87**, 137.
- Finlay, C. C. & Jackson, A., 2003. Equatorially dominated magnetic field change at the surface of Earth's core, *Science*, **300**, 2084–2086.

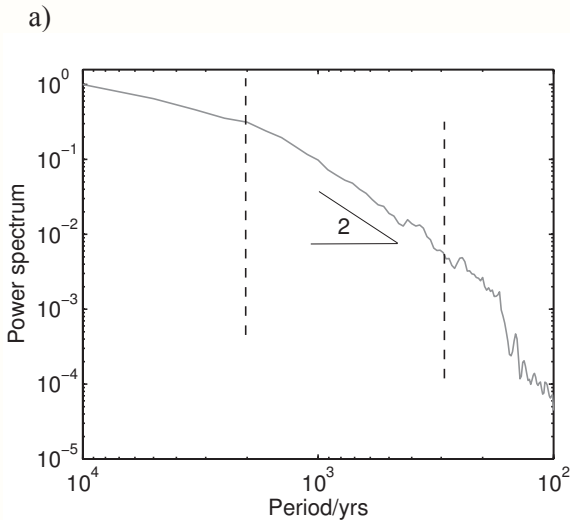
- Finlay, C. C., Maus, S., Beggan, C., Hamoudi, M., Lowes, F. J., Olsen, N., & Thébault, E., 2010. Evaluation of candidate geomagnetic field models for IGRF-11, *Earth, Planets, Space*, p. (submitted to EPS).
- Finlay, C. C., Jackson, A., Gillet, N., & Olsen, N., 2012. Core surface magnetic field evolution 2000–2011, *Geophys. J. Int.*, **189**, 761–781.
- Friis-Christensen, E., Lühr, H., & Hulot, G., 2006. *Swarm*: A constellation to study the Earth's magnetic field, *Earth, Planets, Space.*, **58**, 351–358.
- Gallet, Y., Hulot, G., Chulliat, A., & Genevey, A., 2009. Geomagnetic field hemispheric asymmetry and archeomagnetic jerks, *Earth Planet. Sci. Lett.*, **284**, 179–186.
- Genevey, A., Gallet, Y., Rosen, J., & LeGoff, M., 2009. Evidence for rapid geomagnetic field intensity variations in western Europe over the past 800 years from new French archeointensity data, *Earth Planet. Sci. Lett.*, pp. 132–143.
- Gillet, N., Pais, M. A., & Jault, D., 2009. Ensemble inversion of time-dependent core flow models, *Geochem. Geophys. Geosyst.*, **10**, doi:10.1029/2008GC002290.
- Gillet, N., Jault, D., Finlay, C., & Olsen, N., in prep. Stochastic modelling of the earth's magnetic field: inversion for covariances over the observatory era, *Geochem. Geophys. Geosyst.*.
- Gubbins, D., 1996. A formalism for the inversion of geomagnetic data for core motions with diffusion, *Phys. Earth Planet. Int.*, **98**, 193–206.
- Gubbins, D. & Roberts, N., 1983. Use of the frozen flux approximation in the interpretation of archeomagnetic and paleomagnetic data, *Geophys. J. R. Astr. Soc.*, **73**, 675–687.
- Gubbins, D., Willis, A. P., & Sreenivasan, B., 2007. Correlation of earth's magnetic field with lower mantle thermal and seismic structure, *Phys. Earth Planet. Int.*, **162**, 256–260.
- Hide, R., 2000. Angular momentum fluctuations within the earth's liquid core and torsional oscillations of the core-mantle system, *Geophys. J. Int.*, **1423**, 777–786.
- Holme, R. & Olsen, N., 2006. Core-surface flow modelling from high resolution secular variation, *Geophys. J. Int.*, **166**, 518–528.
- Holme, R., Olsen, N., & Bairstow, F. L., 2011. *Geophys. J. Int.*, **186**, 521–528.

- Hulot, G. & LeMouél, J., 1994. A statistical approach to earth's main magnetic field, *Phys. Earth Planet. Int.*, **82**, 167–183.
- Jackson, A., 1997. Time-dependency of tangentially geostrophic core surface motions, *Phys. Earth Planet. Int.*, **103**, 293–311.
- Jackson, A., 2003. Intense equatorial flux spots on the surface of Earth's core, *Nature*, **424**, 760–763.
- Jackson, A., Jonkers, A. R. T., & Walker, M. R., 2000. Four centuries of geomagnetic secular variation from historical records, *Phil. Trans. R. Soc. Lond. A*, **358**, 957–990.
- Jault, D., Gire, C., & LeMouél, J. L., 1988. Westward drift, core motions and exchanges of angular momentum between core and mantle, *Nature*, **333**, 353–356.
- Jaynes, E. T., 1957. Information theory and statistical mechanics, *Phys. Rev. Lett.*, **106(4)**, 620–630.
- Jonkers, A. R. T., Jackson, A., & Murray, A., 2003. Four centuries of geomagnetic data from historical records, *Rev. Geophys.*, **41**, 1006 doi:10.1029/2002RG000115.
- Kono, M. & Roberts, P. H., 2002. Recent geodynamo simulations and observations of the geomagnetic field, *Rev. Geophys.*, **40**, 1013, doi:10.1029/2000RG00102.
- Korte, M., Genevey, A., Constable, C., Donadini, F., & Holme, R., 2011. Reconstructing the holocene geomagnetic field, *Earth Planet. Sci. Lett.*, **312**, 497–505.
- Kuang, W., Tangborne, A., Jiang, W., Liu, D., & Sabaka, T., 2009. Constraining a numerical geodynamo model with 100 years of surface observations, *Geophys. J. Int.*, **179**, 1458–1468.
- Lesur, V., Wardinski, I., Rother, M., & Mandea, M., 2008. GRIMM: the GFZ reference internal magnetic model based on vector satellite and observatory data, *Geophys. J. Int.*, **173**, 382–394.
- Lesur, V., Wardinski, I., Hamoudi, M., & Rother, M., 2010. The second generation of the GFZ reference internal magnetic model: GRIMM-2, *Earth. Planet. Sp.*, **62**, 765–773.
- Li, K., Jackson, A., & Livermore, P., 2011. Variational data assimilation for the initial-value dynamo problem, *Phys. Rev. E*, **056321**, 1–16.

- Lowes, F. J., 1974. Spatial power spectrum of the main geomagnetic field, and extrapolation to the core, *Geophys. J. R. Astr. Soc.*, **36**, 717–730.
- Neukirch, L., Tarduno, J., Huffman, T., Watkeys, M., Scribner, C., & Cottrell, R., 2012. An archeomagnetic analysis of burnt grain bin floors from ca. 1200 to 1250 ad iron-age south africa, *Phys. Earth Planet. Int.*, **190**(4), 71–79.
- Olsen, N. & Manda, M., 2008. Rapidly changing flow in the Earth's core, *Nature Geosciences*, **1**, 390–394.
- Olsen, N., Manda, M., Sabaka, T. J., & Tø ffer Clausen, L., 2010. The CHAOS-3 geomagnetic field model and candidate models for the 11th generation igrf, **62**, 719–727.
- Olsen, N., Lühr, H., & Sabaka, T., 2012. The chaos-4 geomagnetic field model, *Geophys. J. Int.*, **149**, 454–462.
- Olson, P. & Deguen, R., 2012. Eccentricity of the geomagnetic dipole caused by lopsided inner core growth, *Nature Geosciences*, p. (in press).
- Olson, P., Christensen, U., & Driscoll, P. E., 2012. From superchrons to secular variation: A broadband dynamo frequency spectrum for the geomagnetic dipole, *Earth Planet. Sci. Lett.*, **319**, 75–82.
- Pais, M. & Hulot, G., 2000. Length of day variations, torsional oscillations and inner core super-rotation, *Phys. Earth Planet. Int.*, **118**, 291–316.
- Schaeffer, N. & Pais, M., 2011. On symmetry and anisotropy of earth-core flows, *Geophys. Res. Lett.*, **118**, DOI : 10.1029/2011GL046888.
- Silva, L. & Hulot, G., 2012. Investigating the 2003 geomagnetic jerk by simultaneous inversion of the secular variation and acceleration for both the core flow and its acceleration, *Phys. Earth Planet. Int.*, **198**, 28–50.
- Smirnov, A. V., Tarduno, J. A., & Evans, D. A. D., 2011. Evolving core conditions ca. 2 billion years ago detected by paleosecular variation, *Phys. Earth Planet. Int.*, **187**, 225–231.
- Wardinski, I. & Lesur, V., 2012. An extended version of the c3fm geomagnetic field model: application of a continuous frozen-flux constraint, *Geophys. J. Int.*, **189**, 1409–1420.

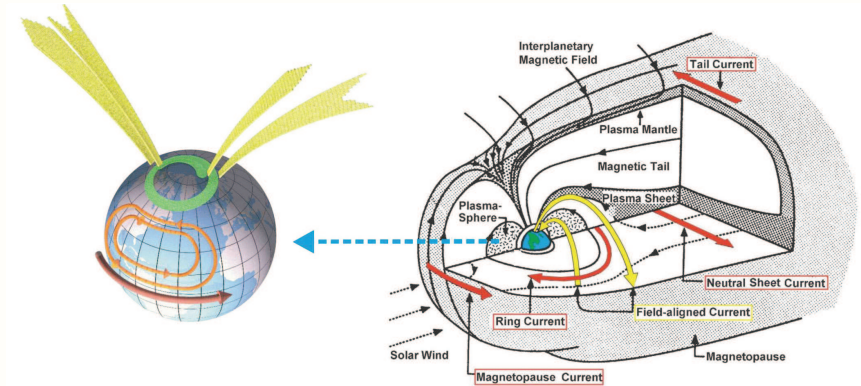
- Zhang, K. & Gubbins, D., 1993. Convection in a rotating spherical fluid shell with inhomogeneous temperature boundary conditions at infinite Prandtl number, *J. Fluid Mech.*, **250**, 209–232.
- Ziegler, L. B., Constable, C. G., Johnson, C. L., & Tauxe, L., 2011. Pad2m: a penalized maximum likelihood model of the 0-2ma palaeomagnetic axial dipole moment, *Geophys. J. Int.*, **184**, 1069–1089.

Temporal spectrum for Holocene sediments



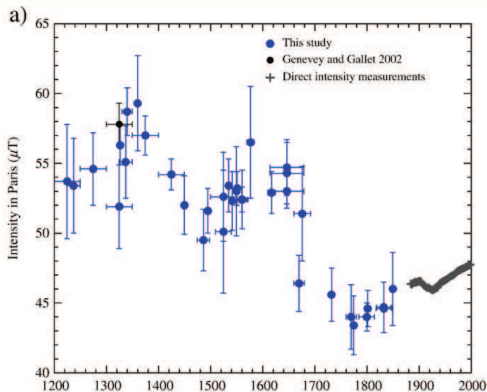
Spectrum of field variations derived from Holocene lake sediment records

Wider geomagnetic environment



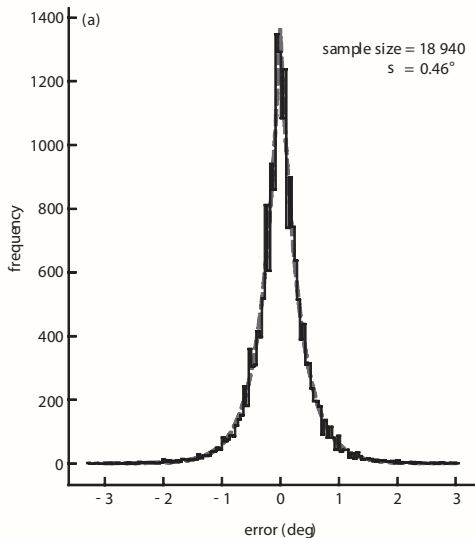
Schematic of electrical currents in the near-Earth environment, produced by interactions with the solar wind.

Example: French intensity records (past 800 yrs)



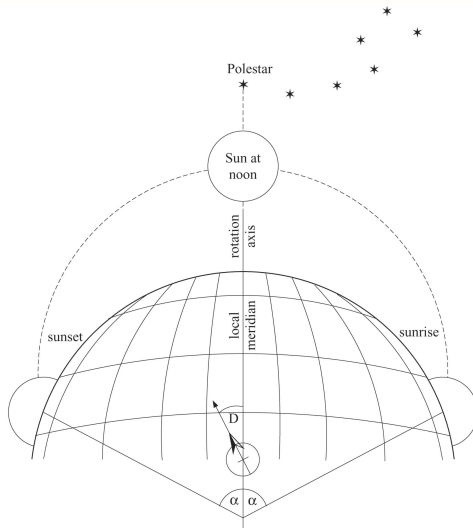
: From [Genevey et al. \(2009\)](#): A high quality, well dated, series of archeointensity determinations spanning the past 800 years in France.

Accuracy of maritime declination measurements



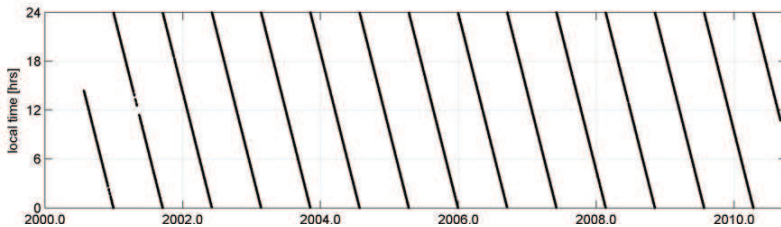
Distribution of deviations of Declination measurements from daily mean, when more than one measurement taken on a certain day. From [Jackson et al. \(2000\)](#)

Determination of declination by mariners



Determinations of declination by mariners. From [Jonkers et al. \(2003\)](#).

CHAMP Orbit



Local time evolution of the ascending node of the CHAMP orbit.

Decay of CHAMP Orbit in 2009

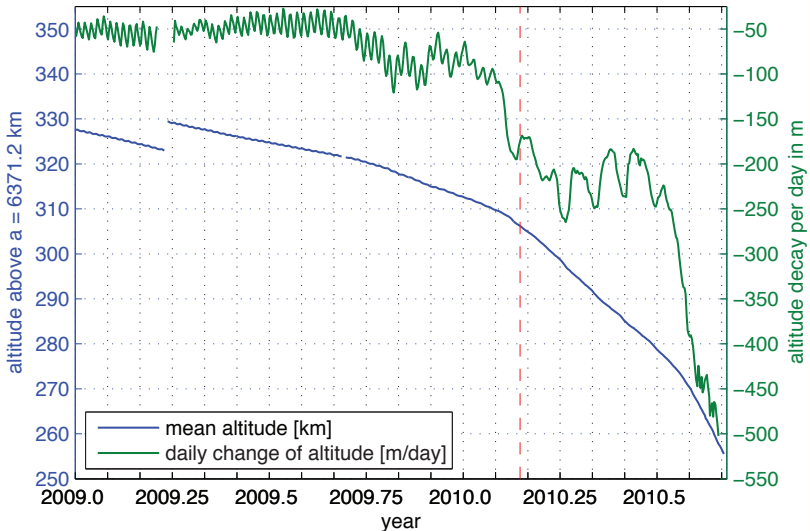


Fig 2.13: Decay of CHAMP altitude in 2009 and 2010. (Plot courtesy of Nils Olsen.)

Spatial spectrum of the present field: Core & Crust

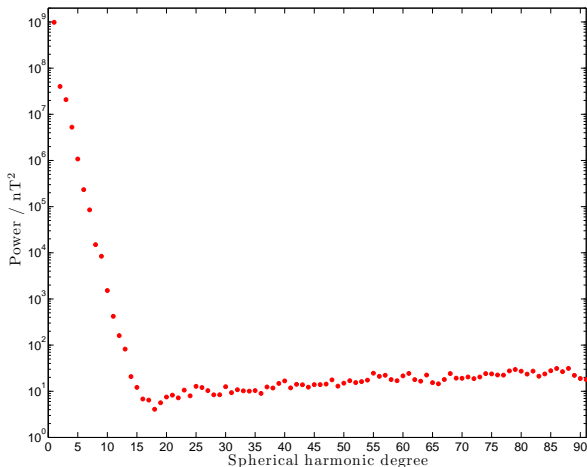


Fig 2.14: Spatial spectrum of geomagnetic field in 2010 at Earth's surface. From the CHAOS-4a model by [Olsen et al. \(2012\)](#) derived from low altitude CHAMP observations.

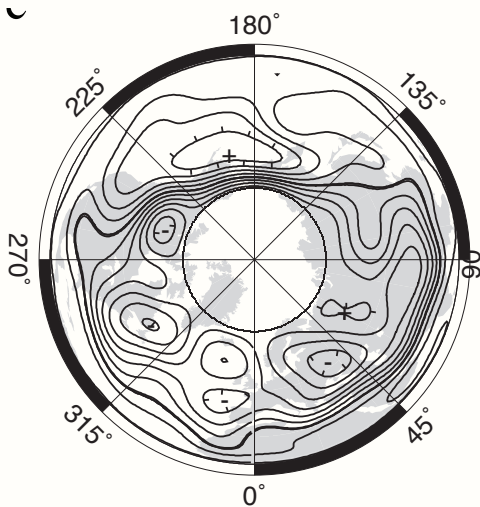
Change in radial field over past 400 years

B_r at Earth's surface from 1590.0 to 1990.0 from the *gufm1* model of [Jackson et al. \(2000\)](#) : units μT

Downward continuation of radial field to core surface

Fig 1.15: Change in B_r during downward continuation (Credit: S. Gibbons)

Stronger assumption: Quasi-geostrophic flow

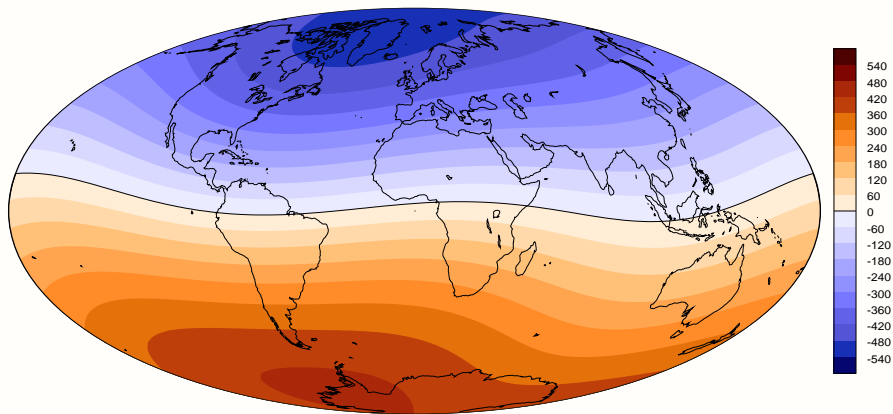


Example quasi-geostrophic core flow derived using the method of [Gillet et al. \(2009\)](#)). From [Finlay et al. \(2010\)](#), courtesy of A. Pais.

Holocene evolution of radial field at the core surface

Fig 4.2: B_r at core surface, 8000BC-1500AD, CALS10k.1b (Korte et al., 2011): units μT

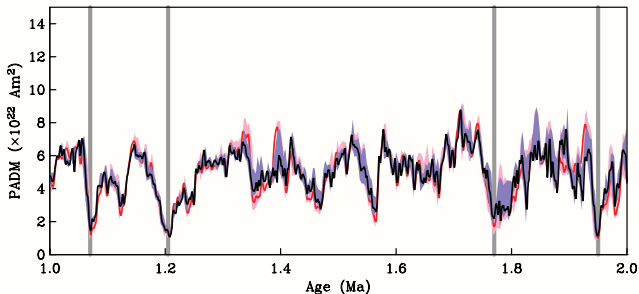
- High latitude flux lobes usually near edge of tangent cylinder.
- Patches can oscillate/drift, but often short-lived (Amit et al., 2011).



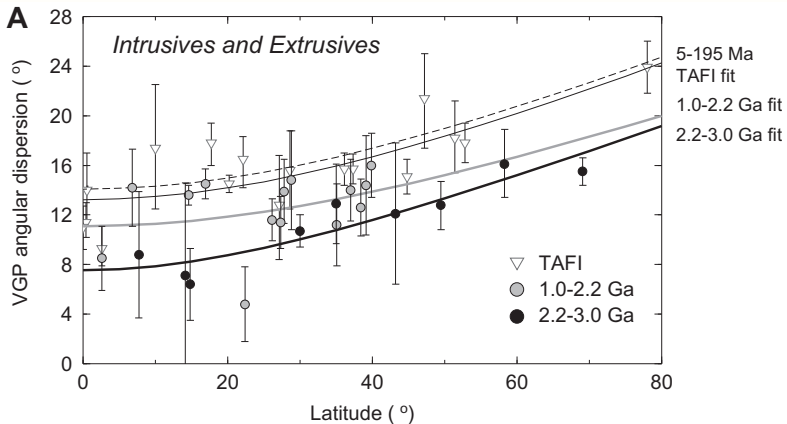
Radial field at the core surface to degree 2 (equivalent to eccentric dipole model) in 400BC. Note offset towards the western hemisphere.

Other recent highlights - long time scales

- [Smirnov et al. \(2011\)](#): ancient paleosecular variation records suggest field more dipolar 2 - 3.5 billion years ago.
Possible signature of a long-term change in core conditions?
- [Ziegler et al. \(2011\)](#): New model of axial dipole moment for past 2Myrs.
Slightly bimodal distribution - implications for geodynamo?

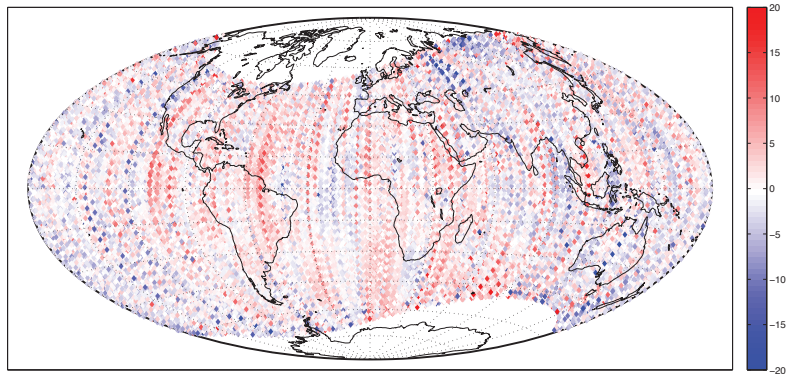


Axial dipole moment from PADM2M ([Ziegler et al., 2011](#)) for 1-2Myrs BP.



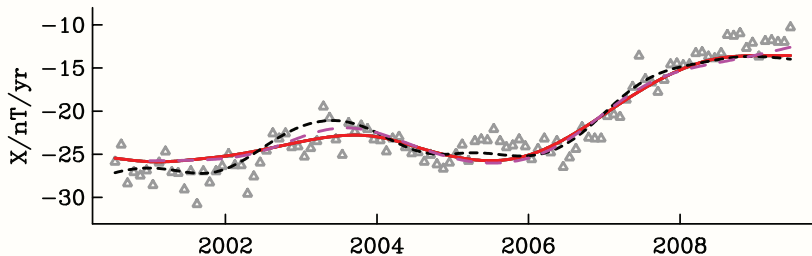
Variations in VGP dispersion - from [Smirnov et al. \(2011\)](#).

Fit to satellite data : CHAMP Y component in 2008



Residuals between *gufm-sat-E3* (Finlay et al., 2012) and CHAMP vector data (Y component) in 2008. Units are nT .

Fit to observatory data: dX/dt at KOU



Comparison of observed and modelled rate of change of X field components at Kourou, French Guyana. Observations are annual differences of month means (grey triangles). Red solid line is *gufm-sat-E3* (Finlay et al., 2012), black dashed line is *CHAOS-3* (Olsen et al., 2010) and pink dashed line is *GRIMM-2* (Lesur et al., 2010).

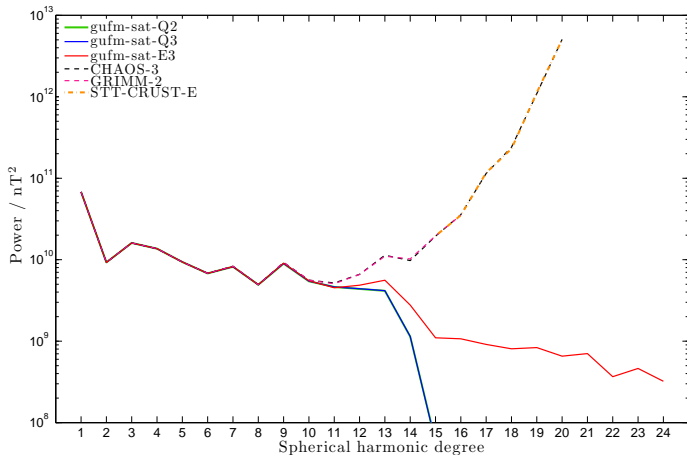
Core field modelling: Entropy regularization

- Jaynes (1957) set out the rationale for using maximum entropy to allocate probabilities in the absence of other information:
- "the maximum-entropy estimate ... is the least biased estimate possible on the given information; i.e. it is maximally non-committal with regard to missing information"
- Often applied to reconstruction of images from incomplete and noisy data e.g.in astronomy, image processing and medical tomography.
- **In Geomagnetism:**
 - (i) Assumes there is a finite amount of magnetic flux.
 - (ii) All possible arrangements assumed equally likely before the data arrives.
 - (iii) Consideration of all possible combinations $\Rightarrow x \ln x$ factor.

Evolution of radial field at the core surface

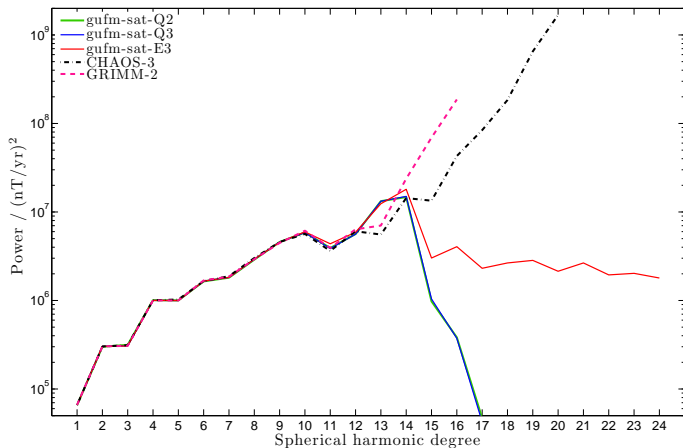
B_r at core surface 2000-2010, *gufm-sat-E3* [Finlay et al. \(2012\)](#) : units μT

MF spectra



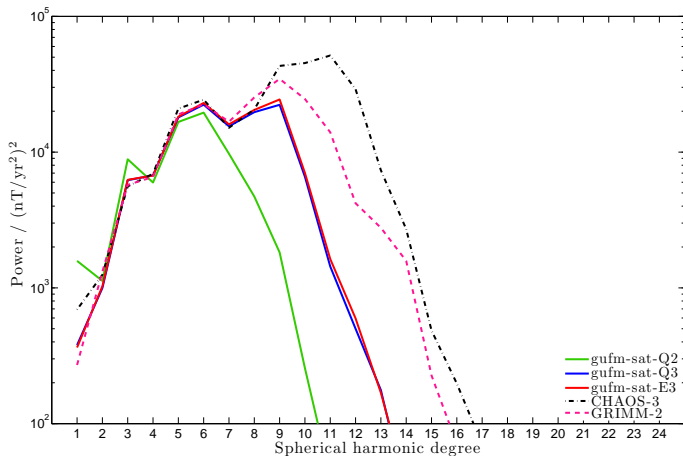
Comparison of MF spectra in 2005.0.

SV spectra



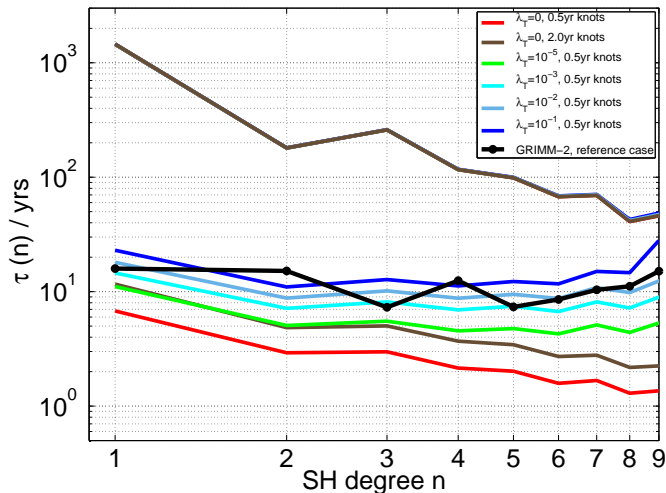
Comparison of SV spectra in 2005.0.

SA spectra



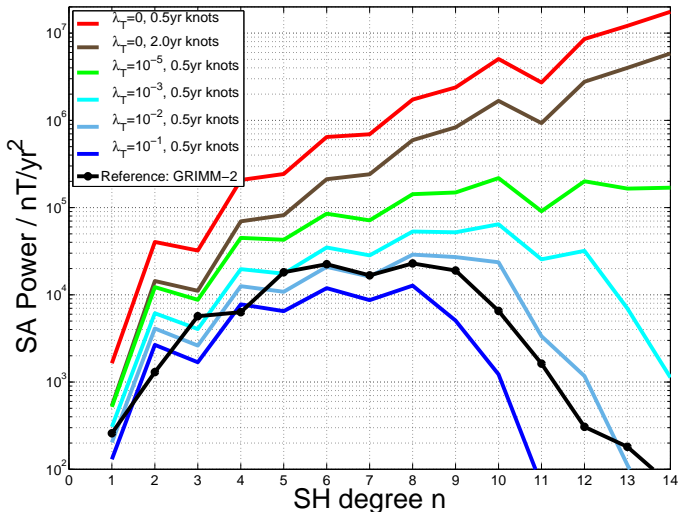
Comparison of SA spectra in 2005.0.

A cautionary note: timescales and regularization



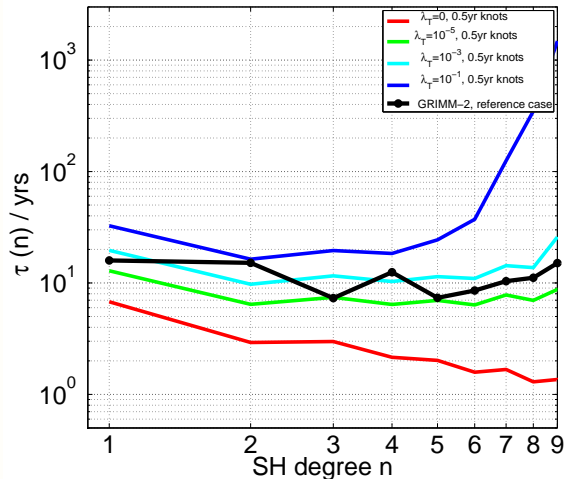
TAU SV regularizing 3rd time derivative

Influence of regularization on secular acceleration



SA spectra at core surface

Influence of regularization on τ SV



TAU SV regularizing 3rd time derivative of Ohmic heating

- Regularizing: OHMIC HEATING

Influence of regularization on secular acceleration

